

Quasiparticle poisoning rate in a superconducting transmon qubit involving Majorana zero modes

Xiaopei Sun^{1,2,*}, Zhaozheng Lyu^{1,2,*†}, Enna Zhuo^{1,2}, Bing Li^{1,2}, Zhongqing Ji¹, Jie Fan¹, Xiaohui Song^{1,4},
Fanning Qu^{1,2,3,4}, Guangtong Liu^{1,2,3,4}, Jie Shen^{1,2,3}, and Li Lu^{1,2,3,4,†}

¹Beijing National Laboratory for Condensed Matter Physics, Institute of Physics, Chinese Academy of Sciences, Beijing 100190, China

²School of Physical Sciences, University of Chinese Academy of Sciences, Beijing 100049, China

³Songshan Lake Materials Laboratory, Dongguan, Guangdong 523808, China

⁴Hefei National Laboratory, Hefei 230088, China

Majorana zero modes have been attracting considerable attention because of their prospective applications in fault-tolerant topological quantum computing. In recent years, some schemes have been proposed to detect and manipulate Majorana zero modes using superconducting qubits. However, manipulating and reading the Majorana zero modes must be kept in the time window of quasiparticle poisoning. In this work, we study the problem of quasiparticle poisoning in a split transmon qubit containing hybrid Josephson junctions involving Majorana zero modes. We show that Majorana coupling will cause parity mixing and 4π Josephson effect. In addition, we obtained the expression of qubit parameter-dependent parity switching rate, and demonstrated that quasiparticle poisoning can be greatly suppressed by reducing E_J/E_C via qubit design.

I. INTRODUCTION

There are many theoretical and experimental explorations along the research direction of realizing fault-tolerant topological quantum computation [1–6]. Among them, a highly regarded scheme is to combine circuit quantum electrodynamics (cQED) with Josephson junctions (JJs) involving Majorana zero modes (MZMs) [7–13]. It is theoretically proposed that a superconducting qubit, such as the Majorana transmon qubit in Ref. [12], can be used to detect and manipulate MZMs. Experimentally, hybrid superconducting qubits have been realized by replacing the superconductor-insulator-superconductor (S-I-S) JJs in conventional superconducting qubits with the JJs based on a variety of materials, such as semiconductor [14–16], van der Waals materials [17,18], and topological materials [19,20]. These hybrid qubits provide a platform for studying Majorana physics and topological quantum computation, since MZMs could be found in the heterojunctions between these materials and s-wave superconductors.

However, both Majorana qubits and superconducting qubits are susceptible to quasiparticle poisoning (QPP) [21–29]. Although the problem of QPP in conventional S-I-S superconducting qubits has been well studied both theoretically [24–27] and experimentally [28–33], QPP in superconducting qubits involving MZMs remains unexplored.

In this work, we consider a split transmon qubit containing MZMs, as schematically depicted in Fig. 1. The parity mixing effect and the 4π Josephson effect caused by Majorana coupling are found in the calculated excitation spectrum of the qubit. We further demonstrate that QPP can be greatly suppressed by reducing E_J/E_C via qubit design.

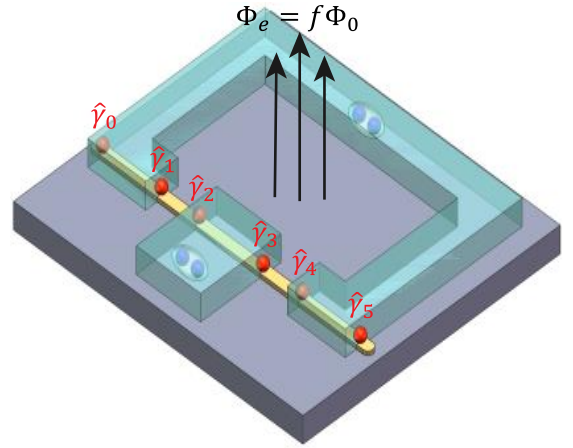


Fig. 1. Schematic of a split transmon qubit with MZMs. Two superconductors (cyan-blue) on a topological nanowire (yellow) form a split transmon with six MZMs (red) in the device.

II. THE TOTAL HAMILTONIAN OF THE MAJORANA-TRANSMON QUBIT

The total hybrid Hamiltonian describing the device in Fig. 1 can be split into four parts [12,25]:

$$\hat{H} = \hat{H}_\phi + \hat{H}_M + \hat{H}_{qp} + \hat{H}_T. \quad (1)$$

The first term describes the regular split transmon Hamiltonian

$$\hat{H}_\phi = 4E_C(\hat{N} - n_g)^2 - E_J(f)\cos\hat{\phi}, \quad f = \frac{\Phi_e}{\Phi_0}, \quad (2)$$

where \hat{N} is the number operator of Cooper pairs, $\hat{\phi}$ is the phase operator, n_g is the dimensionless gate voltage, $\Phi_0 = h/2e$ is the flux quantum, E_C is the charging energy, and the effective Josephson energy $E_J(f)$ is modulated by the external flux Φ_e :

$$E_J(f) = (E_{J0} + E_{J1})|\cos(\pi f)|\sqrt{1 + d^2 \tan^2(\pi f)}, \quad (3)$$

where E_{J0} and E_{J1} are the Josephson energy of two junctions respectively, and $d = (E_{J0} - E_{J1})/(E_{J0} + E_{J1})$ is the junction asymmetry parameter. The

*These authors contribute equally to this work.

† Corresponding authors. Zhaozheng Lyu: lyuzhzh@iphy.ac.cn,

Li Lu: lilu@iphy.ac.cn

qubit frequency of \hat{H}_ϕ is approximately $\omega_p(f) = \sqrt{8E_C E_J(f)}$.

The second term determines the couplings between the MZMs distributed across the Josephson junctions

$$\hat{H}_M = 2iE_{M0}\hat{\gamma}_1\hat{\gamma}_2 \cos\left(\frac{\hat{\phi}_0}{2}\right) + 2iE_{M1}\hat{\gamma}_3\hat{\gamma}_4 \cos\left(\frac{\hat{\phi}_1}{2}\right), \quad (4)$$

where $\hat{\gamma}_1, \hat{\gamma}_2, \hat{\gamma}_3$ and $\hat{\gamma}_4$ are MZMs operators as shown in Fig. 1, E_{M0} and E_{M1} are coupling strengths between the MZMs distributed across the Josephson junctions, $\hat{\phi}_0$ and $\hat{\phi}_1$ describe the phase difference of two junctions respectively:

$$\begin{cases} \hat{\phi}_0 = \pi f - \vartheta - \hat{\phi} \\ \hat{\phi}_1 = \pi f + \vartheta + \hat{\phi} \end{cases}, \quad \tan\vartheta = d \tan(\pi f) \quad (5)$$

The couplings between MZMs on the same electrodes have been ignored in Eq. (4) since they only cause small corrections in the diagonal elements and do not affect our results.

The third term is the sum of the BCS Hamiltonians for quasiparticles in the leads

$$\hat{H}_{qp} = \sum_{j=0,1} \hat{H}_{qp}^j, \quad \hat{H}_{qp}^j = \sum_{n,\sigma} \epsilon_n^j \hat{\alpha}_{n\sigma}^{j\dagger} \hat{\alpha}_{n\sigma}^j, \quad (6)$$

where the index j denotes the superconducting island, $\hat{\alpha}_{n\sigma}^{j\dagger}$ ($\hat{\alpha}_{n\sigma}^j$) are Bogoliubov quasiparticle creation (annihilation) operators with the spin σ ,

and $\epsilon_n^j = \sqrt{(\xi_n^j)^2 + (\Delta^j)^2}$ are quasiparticle energies with ξ_n^j and Δ^j being the single-particle energy level and the superconducting gap in that lead, respectively. In the following we assume equal gaps in the leads $\Delta^j \simeq \Delta$ for simplicity.

The last item is the tunnel Hamiltonian \hat{H}_T which describes quasiparticle tunneling across the junction

$$\begin{aligned} \hat{H}_T &= \sum_{j=0,1} \tilde{t}_j \sum_{n,m,\sigma} \left(e^{i\frac{\hat{\phi}_j}{2}} u_n^j v_m^{j+1} - e^{-i\frac{\hat{\phi}_j}{2}} v_m^{j+1} u_n^j \right) \hat{\alpha}_{n\sigma}^{j\dagger} \hat{\alpha}_{m\sigma}^{j+1} + \text{H.c.} \\ &\simeq \sum_{j=0,1} \tilde{t}_j \sum_{n,m,\sigma} i \sin \frac{\hat{\phi}_j}{2} \hat{\alpha}_{n\sigma}^{j\dagger} \hat{\alpha}_{m\sigma}^{j+1} + \text{H.c.} \end{aligned} \quad (7)$$

where the island $j = 2$ should be identified as the island $j = 0$, \tilde{t}_j are electron tunneling amplitudes between islands j and $j + 1$. \hat{H}_T leads to the interaction between quasiparticles and qubit degrees of freedom and makes possible the transition between two qubit states induced by QPP. Since the tunneling amplitude is usually small $\tilde{t}_j \ll 1$, we can calculate the transition rates by treating \hat{H}_T as a perturbation term.

III. THE SOLUTION OF THE HYBRID QUBIT SYSTEM

In contrast to the regular transmon qubits, the Majorana coupling term \hat{H}_M in Eq. (4) will double the degeneracy of the qubit states, and the charge parity of the qubit will be jointly determined by the quasiparticle parity and the Majorana parity. The Hamiltonian in Eq. (1) can be projected on four different parity states:

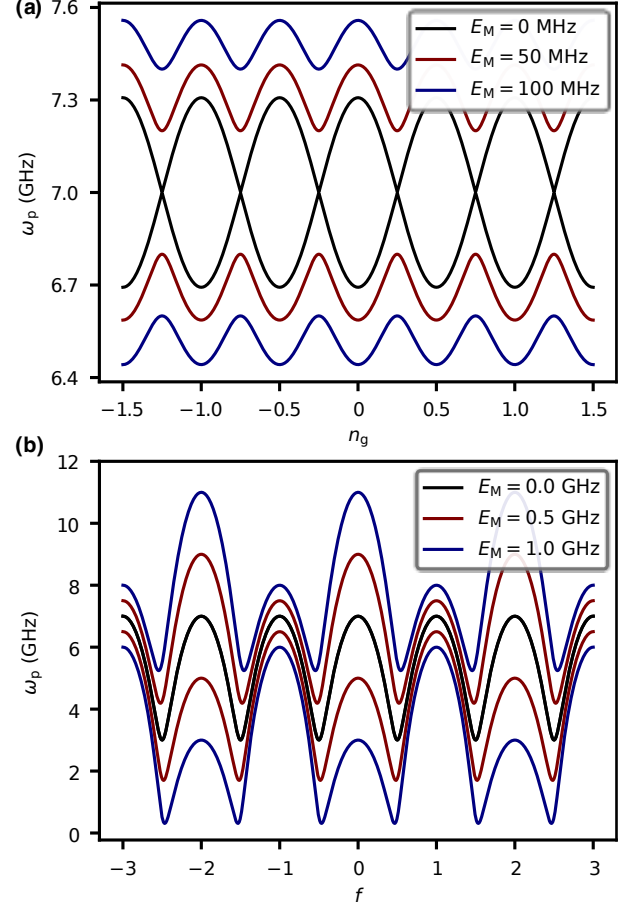


Fig. 2. Calculated excitation spectrum of the Majorana transmon qubit with $E_C = 1$ GHz, $E_J = 8$ GHz, and $d = 0.25$. For simplicity, we denote the average of E_{M1} and E_{M2} as $E_M = (E_{M1} + E_{M2})/2$. (a) The excitation spectrum as a function of gate voltage n_g with $E_M = 0$ (black), $E_M = 50$ MHz (red), and $E_M = 100$ MHz (blue). (b) The excitation spectrum as a function of flux f with $E_M = 0$ (black), $E_M = 0.5$ GHz (red), and $E_M = 1$ GHz (blue).

$$\begin{pmatrix} |\psi_n^e, \{e\}_{qp}, \{e\}_M\rangle \\ |\psi_n^o, \{e\}_{qp}, \{o\}_M\rangle \\ |\psi_n^e, \{o\}_{qp}, \{o\}_M\rangle \\ |\psi_n^o, \{o\}_{qp}, \{e\}_M\rangle \end{pmatrix} \quad (8)$$

where ψ_n^ζ represents the eigenstate of transmon, ζ denotes the total charge parity, n denotes the energy level of the qubit, $\{e\}_{qp}$ ($\{o\}_{qp}$) corresponds to the even (odd) states of the quasiparticles, $\{e\}_M$ consists of the Majorana parity states $|01\rangle$ and $|00\rangle$, $\{o\}_M$ consists of the Majorana parity states $|10\rangle$ and $|11\rangle$. By replacing the Majorana operators in Eq. (4) with the fermion operators (e.g., $-2i\hat{\gamma}_1\hat{\gamma}_2 = \hat{c}_0^\dagger\hat{c}_1 + \hat{c}_1^\dagger\hat{c}_0 + \hat{c}_0^\dagger\hat{c}_1^\dagger + \hat{c}_1\hat{c}_0$), it is straightforward to find that the matrix elements of \hat{H}_M are non-zero only when the two states have different Majorana parities but the same quasiparticle parity

$$\langle \psi_n^\zeta, \{\lambda\}_{qp}, \{\eta\}_M | \hat{H}_M | \psi_n^\zeta, \{\lambda\}_{qp}, \{\eta\}_M \rangle = \sum_{j=0,1} E_{Mj} \langle \psi_n^\zeta | \cos \frac{\hat{\phi}_j}{2} | \psi_n^\zeta \rangle. \quad (9)$$

In the transmon limit $E_J/E_C \gg 1$, we can expand Eq. (2) around $\phi = 0$ up to the second order, and then use the standard harmonic oscillator eigenstates as the qubit states. In order to obtain the analytic expressions for the matrix elements of $\cos(\hat{\phi}_j/2)$, we introduce the displacement operator

$$\hat{D}(\mu) = e^{\mu \hat{a}^\dagger - \mu^* \hat{a}}, \quad (10)$$

where \hat{a} and \hat{a}^\dagger are the annihilation and creation operators respectively. When $\mu = i\sqrt{E_C/\omega_p}$, by using $\hat{\phi} = 2\sqrt{E_C/\omega_p}(\hat{a} + \hat{a}^\dagger)$, we have

$$\hat{D}\left(i\sqrt{E_C/\omega_p}\right) = e^{i\hat{\phi}/2}. \quad (11)$$

Since $\hat{\phi}_j$ is shifted by $\varphi_\pm = \vartheta \pm \pi f$ in Eq. (S6), $\cos(\hat{\phi}_j/2)$ can be expressed as

$$\begin{aligned} \cos\frac{\varphi_\pm + \hat{\phi}}{2} &= \frac{1}{2}\left(e^{i\varphi_\pm/2}e^{i\hat{\phi}/2} + e^{-i\varphi_\pm/2}e^{-i\hat{\phi}/2}\right) \\ &= \frac{1}{2}\left[e^{\frac{i\varphi_\pm}{2}}\hat{D}\left(i\sqrt{\frac{E_C}{\omega_p}}\right) + e^{-\frac{i\varphi_\pm}{2}}\hat{D}\left(-i\sqrt{\frac{E_C}{\omega_p}}\right)\right]. \end{aligned} \quad (12)$$

The matrix elements of $\hat{D}(\mu)$ are [34]:

$$\langle \psi_m | \hat{D}(\mu) | \psi_n \rangle = \begin{cases} e^{-|\mu|^2/2} \frac{m!}{n!} (-\mu^*)^{n-m} L_m^{(n-m)}(|\mu|^2), & m \leq n \\ e^{-|\mu|^2/2} \frac{n!}{m!} (\mu)^{m-n} L_n^{(m-n)}(|\mu|^2), & m \geq n \end{cases} \quad (13)$$

where $L_n^{(l)}$ are the generalized Laguerre polynomials and can be expanded as

$$L_m^{(l)}(x) = \frac{(m+l)!}{m!l!} - \frac{(m+l)!}{(m-1)!(l+1)!}x + \mathcal{O}(x^2). \quad (14)$$

Since $\mu = i\sqrt{E_C/\omega_p} = i(E_C/8E_J)^{1/4} \ll 1$ in the transmon limit $E_J/E_C \gg 1$, we can expand Eq. (12) up to the second order of μ

$$\begin{aligned} \langle \psi_m | \cos\frac{\hat{\phi}_j}{2} | \psi_n \rangle &= \\ &\left[1 - \left(n + \frac{1}{2}\right)\frac{E_C}{\omega_p}\right] \delta_{m,n} \cos\frac{\hat{\phi}_\pm}{2} \\ &- \sqrt{\frac{E_C}{\omega_p}} \left[n\delta_{m,n-1} + (n+1)\delta_{m,n+1}\right] \sin\frac{\hat{\phi}_\pm}{2} \\ &+ \frac{1}{2}\frac{E_C}{\omega_p} \left[\sqrt{n(n-1)}\delta_{m,n-2} + \sqrt{(n+1)(n+2)}\delta_{m,n+2}\right] \cos\frac{\hat{\phi}_\pm}{2}. \end{aligned} \quad (15)$$

For the qubit degrees of freedom we are considering, the quasiparticle term \hat{H}_{qp} can be neglected. And we consider first the solution at ground states and then generalize the result to higher energies. In the basis of Eq. (8), the hybrid Hamiltonian yields the form

$$\hat{H}_Q = \hat{H}_\phi + \hat{H}_M = \frac{1}{2} \begin{pmatrix} \omega_{eo} & \omega_M & & \\ \omega_M & -\omega_{eo} & & \\ & & \omega_{eo} & \omega_M \\ & & \omega_M & -\omega_{eo} \end{pmatrix}, \quad (16)$$

where $\omega_M = 2\langle \psi_0^\zeta, \{\lambda\}_{qp}, \{\eta\}_M | \hat{H}_M | \psi_0^\zeta, \{\lambda\}_{qp}, \{\eta\}_M \rangle$, substituting Eq. (15)

into Eq. (9), we obtain

$$\omega_M \simeq 2 \sum_{j=0,1} E_{Mj} \cos\frac{\pi f - (-1)^j \vartheta}{2}, \quad (17)$$

ω_{eo} is the energy difference between even and odd ground states of the regular transmon. Following Appendix B of Ref. [25], ω_{eo} can be expressed

as

$$\omega_{eo} = \epsilon_0 \cos(2\pi n_g) \simeq 4 \sqrt{\frac{2}{\pi}} \omega_p \left(\frac{8E_J}{E_C}\right)^{\frac{1}{4}} e^{-\sqrt{8E_J/E_C}} \cos(2\pi n_g). \quad (18)$$

The two states corresponding to the eigenvalue $E_0^+ = \omega'_{eo}/2 = \sqrt{\omega_{eo}^2 + \omega_M^2}/2$ are:

$$\begin{cases} |\Psi_0^+, \{e\}_{qp}\rangle = a^+ |\psi_0^e, \{e\}_{qp}, \{e\}_M\rangle + b^+ |\psi_0^o, \{e\}_{qp}, \{o\}_M\rangle \\ |\Psi_0^+, \{o\}_{qp}\rangle = a^+ |\psi_0^e, \{o\}_{qp}, \{o\}_M\rangle + b^+ |\psi_0^o, \{o\}_{qp}, \{e\}_M\rangle \end{cases} \quad (19)$$

and the two states corresponding to the eigenvalue $E_0^- = -\omega'_{eo}/2 = -\sqrt{\omega_{eo}^2 + \omega_M^2}/2$ are:

$$\begin{cases} |\Psi_0^-, \{e\}_{qp}\rangle = a^- |\psi_0^e, \{e\}_{qp}, \{e\}_M\rangle + b^- |\psi_0^o, \{e\}_{qp}, \{o\}_M\rangle \\ |\Psi_0^-, \{o\}_{qp}\rangle = a^- |\psi_0^e, \{o\}_{qp}, \{o\}_M\rangle + b^- |\psi_0^o, \{o\}_{qp}, \{e\}_M\rangle \end{cases} \quad (20)$$

where

$$\begin{aligned} a^\pm &= \frac{\omega_{eo} \pm \omega'_{eo}}{\sqrt{\omega_M^2 + (\omega_{eo} \pm \omega'_{eo})^2}}, \\ b^\pm &= \frac{\omega_M}{\sqrt{\omega_M^2 + (\omega_{eo} \pm \omega'_{eo})^2}}. \end{aligned} \quad (21)$$

$\omega'_{eo} = \sqrt{\omega_{eo}^2 + \omega_M^2}$ is the energy splitting between the hybrid ground states, which indicates an energy splitting of ω_M at the parity crossing at $n_g = 1/4$.

This result agrees well with the calculated spectrum in Ref. [12], thus validating our approach. Following Ref. [25], the solution at the excited state has a similar expression to Eq. (19-21) but with ω_{eo} replaced by the energy splitting at the excited state $\omega_{eo}^{(1)} = -4\omega_{eo}\omega_p/E_C$. Figure 2(a) shows the energy splitting in excitation spectrum caused by the parity mixing effect and Fig. 2(b) shows the 4π Josephson effect. Both these characteristics are crucial criteria for identifying MZMs.

IV. THE PARITY-SWITCHING RATES

Next, we calculate the parity switching rate at the ground state of the hybrid system by using Fermi's golden rule and treating \hat{H}_T as a perturbation term, following Ref. [25], we can write

$$\begin{aligned} \Gamma_{00}^{oe} &= 2\pi \sum_{\kappa'=\pm} \sum_{\{e\}_{qp}} \left\langle \left(|\langle \Psi_0^{\kappa'}, \{e\}_{qp} | \hat{H}_T | \Psi_0^{\kappa}, \{o\}_{qp} \rangle \right|^2 \right. \\ &\quad \left. \times \delta(E_{e,qp} - E_{o,qp} - \omega'_{eo}) \right\rangle_{\kappa, \{o\}_{qp}} \end{aligned} \quad (22)$$

where $E_{o,qp}$ ($E_{e,qp}$) is the total energy of quasiparticles in their initial (final) state $\{o\}_{qp}$ ($\{e\}_{qp}$), and the double angular brackets $\langle \langle \dots \rangle \rangle_{\kappa, \{o\}_{qp}}$ denote averaging over the initial quasiparticle states. In the low-energy regime, substituting Eq. (7), Eq. (19) and Eq. (20) into Eq. (22) and using $\tilde{t}_j^2 \propto E_{jj}$, we can factorize Γ_{00}^{oe} into terms accounting separately for qubit dynamic and quasiparticle kinetics

$$\begin{aligned}
\Gamma_{00}^{oe} &= \sum_{j=0,1} \frac{E_{jj}}{E_j(f)} \left| \langle \psi_0^e | \sin \frac{\hat{\phi}_j}{2} | \psi_0^e \rangle \right|^2 \\
&\quad \times [(2a^+b^+)^2 S_{qp}(0) + (a^+b^- + a^-b^+)^2 S_{qp}(\omega'_{eo})] \\
&= \sum_{j=0,1} \frac{E_{jj}}{E_j(f)} \left| \langle \psi_0^e | \sin \frac{\hat{\phi}_j}{2} | \psi_0^e \rangle \right|^2 \\
&\quad \times \left[\frac{\omega_M^2}{\omega_M^2 + \omega_{eo}^2} S_{qp}(0) + \frac{\omega_{eo}^2}{\omega_M^2 + \omega_{eo}^2} S_{qp}(\omega'_{eo}) \right] \\
&= \frac{E_{J0} + E_{J1}}{2E_j(f)} \left(1 - \frac{\omega_p^2(f)}{\omega_p^2(0)} \right) \\
&\quad \times \left[\frac{\omega_M^2}{\omega_M^2 + \omega_{eo}^2} S_{qp}(0) + \frac{\omega_{eo}^2}{\omega_M^2 + \omega_{eo}^2} S_{qp}(\omega'_{eo}) \right]
\end{aligned} \tag{23}$$

where, going from the second to the third line, we calculate the matrix elements of $\sin(\hat{\phi}_j/2)$ in a similar way to the calculation of Eq. (15), and S_{qp} is the quasiparticle current spectral density which can be expressed as {Citation}:

$$S_{qp}(\omega) = \frac{16E_j(f)}{\pi} e^{-\Delta/T} e^{\omega/2T} K_0 \left(\frac{|\omega|}{2T} \right), \tag{24}$$

where T is the temperature, K_0 is the modified Bessel function of the second kind.

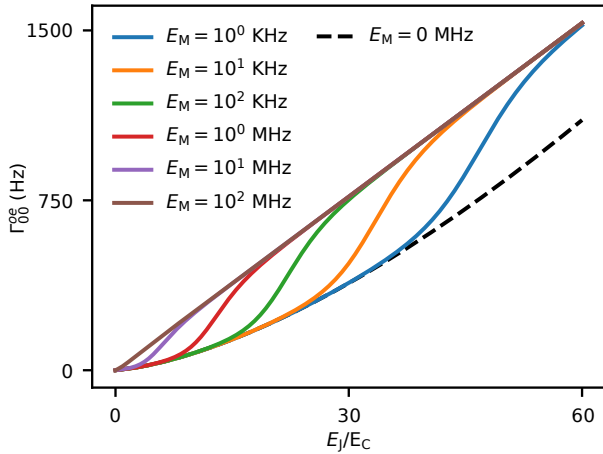


Fig. 3. The parity-switching rate at the ground state of the symmetric split transmon as a function of E_j/E_C with $E_C = 0.2$ GHz, $n_g = 0$, $f = 0.25$, $T = 100$ mK, $\Delta = 161$ μ eV and for different E_M . The black dashed line corresponds to the regular split transmon (i.e. $E_M = 0$).

We remind that $\omega'_{eo} = \sqrt{\omega_{eo}^2 + \omega_M^2}$. It is straightforward to find that when $\omega_M = 0$, Eq. (23) is in agreement with the result of the regular split transmon in Ref. [25]. The parity-switching rate at the excited state Γ_{11}^{oe} can also be calculated by a similar way, and has a similar expression to Eq. (23) in the transmon limit but with ω_{eo} replaced by the energy splitting at the excited state $\omega_{eo}^{(1)} = -4\omega_{eo}\omega_p/E_C$.

Since ω_{eo} is exponentially suppressed by the increasing E_j/E_C as shown in Eq. (18), the parity-switching rates at the same qubit states (i.e., Γ_{00}^{oe} and Γ_{11}^{oe}) are strongly correlated with the qubit design E_j/E_C , as shown in Fig. 3. Therefore, we can suppress Γ_{00}^{oe} and Γ_{11}^{oe} by reducing E_j/E_C via qubit design.

V. SUMMARY

In this work, we have studied the QPP in a split transmon qubit involving Majorana-based Josephson effect. By approximating the transmon qubit as a harmonic oscillator, we have solved the Hamiltonian of this hybrid system analytically and demonstrated the parity mixing effect and the 4π Josephson effect caused by Majorana coupling. These two phenomena could provide an important evidence for MZMs in microwave experiments. In addition, we have derived the expression of qubit parameter-dependent parity-switching rate, and showed that QPP can be greatly suppressed by reducing E_j/E_C via qubit design.

ACKNOWLEDGMENTS

This work was supported by the National Basic Research Program of China through MOST Grant Nos. 2016YFA0300601, 2017YFA0304700 and 2015CB921402; by NSFC through Grant Nos. 11527806, 92065203, 12074417, 11874406 and 11774405; by the Strategic Priority Research Program B of the Chinese Academy of Sciences through Grants Nos. XDB33010300, DB28000000 and XDB07010100; by the Synergetic Extreme Condition User Facility (SECUF) which is sponsored by the National Development and Reform Commission; by the NSFC for Young Scholars through Grant No. E2J1141; and by the Innovation Program for Quantum Science and Technology through Grant No. 2021ZD302600.

- [1] A. Y. Kitaev, Unpaired Majorana Fermions in Quantum Wires, *Phys.-Uspekhi* **44**, 131 (2001).
- [2] S. D. Sarma, M. Freedman, and C. Nayak, Majorana Zero Modes and Topological Quantum Computation, *Npj Quantum Inf.* **1**, 15001 (2015).
- [3] L. Fu and C. L. Kane, Superconducting Proximity Effect and Majorana Fermions at the Surface of a Topological Insulator, *Phys. Rev. Lett.* **100**, 096407 (2008).
- [4] A. Cook and M. Franz, Majorana Fermions in a Topological-Insulator Nanowire Proximity-Coupled to an s-Wave Superconductor, *Phys. Rev. B* **84**, 201105 (2011).
- [5] R. M. Lutchyn, J. D. Sau, and S. D. Sarma, Majorana Fermions and a Topological Phase Transition in Semiconductor-Superconductor Heterostructures, *Phys. Rev. Lett.* **105**, 077001 (2010).
- [6] J. D. Sau, R. M. Lutchyn, S. Tewari, and S. D. Sarma, Generic New Platform for Topological Quantum Computation Using Semiconductor Heterostructures, *Phys. Rev. Lett.* **104**, 040502 (2010).
- [7] C. Müller, J. Bourassa, and A. Blais, Detection and Manipulation of Majorana Fermions in Circuit QED, *Phys. Rev. B* **88**, 235401 (2013).
- [8] M. C. Dartiailh, T. Kontos, B. Douçot, and A. Cottet, Direct Cavity

- Detection of Majorana Pairs, *Phys. Rev. Lett.* **118**, 126803 (2017).
- [9] M. Trif and P. Simon, Braiding of Majorana Fermions in a Cavity, *Phys. Rev. Lett.* **122**, 236803 (2019).
- [10] L. C. Contamin, M. R. Delbecq, B. Douçot, A. Cottet, and T. Kontos, Hybrid Light-Matter Networks of Majorana Zero Modes, *Npj Quantum Inf.* **7**, 171 (2021).
- [11] D. Pekker, C. Y. Hou, V. E. Manucharyan, and E. Demler, Proposal for Coherent Coupling of Majorana Zero Modes and Superconducting Qubits Using the 4π Josephson Effect, *Phys Rev Lett* **111**, 10 (2013).
- [12] E. Ginossar and E. Grosfeld, Microwave Transitions as a Signature of Coherent Parity Mixing Effects in the Majorana-Transmon Qubit, *Nat. Commun.* **5**, 4772 (2014).
- [13] J. Ávila, E. Prada, P. San-Jose, and R. Aguado, Majorana Oscillations and Parity Crossings in Semiconductor Nanowire-Based Transmon Qubits, *Phys. Rev. Res.* **2**, 033493 (2020).
- [14] G. de Lange, B. van Heck, A. Bruno, D. J. van Woerkom, A. Geresdi, S. R. Plissard, E. P. Bakkers, A. R. Akhmerov, and L. DiCarlo, Realization of Microwave Quantum Circuits Using Hybrid Superconducting-Semiconducting Nanowire Josephson Elements, *Phys Rev Lett* **115**, 127002 (2015).
- [15] T. W. Larsen, K. D. Petersson, F. Kuemmeth, T. S. Jespersen, P. Krogstrup, J. Nygard, and C. M. Marcus, Semiconductor-Nanowire-Based Superconducting Qubit, *Phys Rev Lett* **115**, 127001 (2015).
- [16] L. Casparis *et al.*, Superconducting Gatemon Qubit Based on a Proximitized Two-Dimensional Electron Gas, *Nat Nanotechnol* **13**, 915 (2018).
- [17] J. I. Wang *et al.*, Coherent Control of a Hybrid Superconducting Circuit Made with Graphene-Based van Der Waals Heterostructures, *Nat Nanotechnol* **14**, 120 (2019).
- [18] M. Mergenthaler, A. Nersisyan, A. Patterson, M. Esposito, A. Baumgartner, C. Schönberger, G. A. D. Briggs, E. A. Laird, and P. J. Leek, Circuit Quantum Electrodynamics with Carbon-Nanotube-Based Superconducting Quantum Circuits, *Phys. Rev. Appl.* **15**, 064050 (2021).
- [19] K.-L. Chiu *et al.*, Flux Tunable Superconducting Quantum Circuit Based on Weyl Semimetal MoTe₂, *Nano Lett.* **20**, 8469 (2020).
- [20] T. W. Schmitt *et al.*, Integration of Topological Insulator Josephson Junctions in Superconducting Qubit Circuits, *Nano Lett.* **22**, 2595 (2022).
- [21] J. M. Martinis, M. Ansmann, and J. Aumentado, Energy Decay in Superconducting Josephson-Junction Qubits from Nonequilibrium Quasiparticle Excitations, *Phys. Rev. Lett.* **103**, 097002 (2009).
- [22] D. Rainis and D. Loss, Majorana Qubit Decoherence by Quasiparticle Poisoning, *Phys. Rev. B* **85**, 174533 (2012).
- [23] T. Karzig, W. S. Cole, and D. I. Pikulin, Quasiparticle Poisoning of Majorana Qubits, *Phys. Rev. Lett.* **126**, 057702 (2021).
- [24] G. Catelani, J. Koch, L. Frunzio, R. J. Schoelkopf, M. H. Devoret, and L. I. Glazman, Quasiparticle Relaxation of Superconducting Qubits in the Presence of Flux, *Phys. Rev. Lett.* **106**, 077002 (2011).
- [25] G. Catelani, R. J. Schoelkopf, M. H. Devoret, and L. I. Glazman, Relaxation and Frequency Shifts Induced by Quasiparticles in Superconducting Qubits, *Phys. Rev. B* **84**, 064517 (2011).
- [26] G. Catelani, S. E. Nigg, S. M. Girvin, R. J. Schoelkopf, and L. I. Glazman, Decoherence of Superconducting Qubits Caused by Quasiparticle Tunneling, *Phys. Rev. B* **86**, 184514 (2012).
- [27] G. Catelani, Parity Switching and Decoherence by Quasiparticles in Single-Junction Transmons, *Phys. Rev. B* **89**, 094522 (2014).
- [28] K. Serniak, M. Hays, G. de Lange, S. Diamond, S. Shankar, L. D. Burkhardt, L. Frunzio, M. Houzet, and M. H. Devoret, Hot Nonequilibrium Quasiparticles in Transmon Qubits, *Phys. Rev. Lett.* **121**, 157701 (2018).
- [29] K. Serniak, S. Diamond, M. Hays, V. Fatemi, S. Shankar, L. Frunzio, R. J. Schoelkopf, and M. H. Devoret, Direct Dispersive Monitoring of Charge Parity in Offset-Charge-Sensitive Transmons, *Phys. Rev. Appl.* **12**, 014052 (2019).
- [30] R. Barends *et al.*, Minimizing Quasiparticle Generation from Stray Infrared Light in Superconducting Quantum Circuits, *Appl. Phys. Lett.* **99**, 113507 (2011).
- [31] L. Sun *et al.*, Measurements of Quasiparticle Tunneling Dynamics in a Band-Gap-Engineered Transmon Qubit, *Phys. Rev. Lett.* **108**, 230509 (2012).
- [32] S. Gustavsson *et al.*, Suppressing Relaxation in Superconducting Qubits by Quasiparticle Pumping, *Science* **354**, 1573 (2016).
- [33] W. Uilhoorn, J. G. Kroll, A. Bargerbos, S. D. Nabi, C.-K. Yang, P. Krogstrup, L. P. Kouwenhoven, A. Kou, and G. de Lange, Quasiparticle Trapping by Orbital Effect in a Hybrid Superconducting-Semiconducting Circuit, *ArXiv210511038 Cond-Mat* (2021).
- [34] J. N. Hollenhorst, Quantum Limits on Resonant-Mass Gravitational-Radiation Detectors, *Phys. Rev. D* **19**, 1669 (1979).